Kulkarni *et al.*
*Journal of Engineering and Applied Science* (2023) 70:29
https://doi.org/10.1186/s44147-023-00202-y

Journal of Engineering and Applied Science

RESEARCH Open Access

# Anti-wear (AW) and extreme-pressure (EP) behavior of jojoba oil dispersed with green additive $CaCO_3$ nanoparticles

Trishul Kulkarni[1*], Bhagwan Toksha[2], Aniruddha Chatterjee[2], Jitendra Naik[3] and Arun Autee[1]

*Correspondence:
trishulkulkarni@gmail.com

[1] Department of Mechanical Engineering, Maharashtra Institute of Technology, Aurangabad 431010, India
[2] Centre for Advanced Materials Research and Technology, Maharashtra Institute of Technology, Aurangabad 431010, India
[3] University Institute of Chemical Technology, Kavayitri Bahinabai Chaudhari North Maharashtra University, Jalgaon 425001, India

## Abstract

Lubricating approaches involving nanoparticles have a significant role in reducing friction and wear. Reducing friction is crucial for preserving energy, minimizing emissions, and protecting the environment. The present experimental study investigates green nano-lubricants prepared by dispersing various concentrations of $CaCO_3$ nanoparticles in jojoba oil. The aim of the study is to assess the usability of a bio-sourced alternative nanolubricant to depleting conventional lubricants. The role of nanoparticle concentration and thermo-physical properties in improving the lubrication properties of jojoba oil was thoroughly investigated in the present study. The anti-wear and extreme-pressure behavior of jojoba oil dispersed with $CaCO_3$ nanoparticles were evaluated as per the ASTM D4172 and ASTM D2783 test standards. The coefficient of friction, wear scar diameter, last non-seizure load, initial seizure load, weld point load, and load wear index of each sample were assessed. Compared with pure jojoba oil, the addition of $CaCO_3$ nanoparticles in jojoba oil revealed remarkable anti-wear and extreme-pressure properties with significant improvements in the last non-seizure load, initial seizure load, weld point load, and load wear index, the average friction coefficient and the average wear scar diameter of the steel balls decreased by as much as 34.1% and 40.2%, respectively.

**Keywords:** Anti-wear, Extreme pressure, Load wear index, Nanolubricant, Jojoba oil, $CaCO_3$ nanoparticles

## Introduction

Mineral oils are crucial commodities in the industrialized twenty-first century and have many uses that make them indispensable. Most of the lubricants used in the industry are derived from petroleum-based mineral oils [1]. The primary issue is the direct loss of the used lubricants in the soil and water, whereas volatile lubricants pollute the air. Many of these lubricants released into the atmosphere are harmful to the environment. The necessity of biodegradable lubricants to replace traditional mineral oil lubricants has been emphasized by many researchers [2, 3]. Bio-based oils have experienced a revival more recently as a part of efforts to reduce the use of petroleum-based lubricants due to concerns about environmental protection, the depletion of oil reserves, and rises in oil

prices. In this scenario, researchers' top priority is the use of environmentally friendly oils in place of mineral and synthetic oils [4, 5].

Vegetable-based oils are preferred as a base stock for lubricants since they are biodegradable, non-toxic, and hence safe for the environment in comparison to petroleum-based oils. In addition to being non-toxic, vegetable oils also have a high flash point, a high viscosity index, and relatively low volatility as triglyceride molecules have a large molecular weight [6]. Various studies have reported the use of jojoba oil [7–10], rapeseed oil [11–13], palm oil [14], karanja oil [15, 16], sunflower oil [17, 18], soybean oil [19–21], pongamia oil [22, 23], coconut oil [24, 25], jatropha oil [26, 27], and castor oil [28, 29] as potential lubricants in comparison to petroleum-based lubricants. However, vegetable oil's main disadvantage is its low thermal and oxidative stability, which has limited its usage as a lubricant at high temperatures.

Lubricants containing vegetable oil as the base oil must have anti-wear (AW) and extreme pressure (EP) additives as friction and wear are relatively high in mixed/boundary lubrication situations and under extreme loads [30]. Traditional AW and EP additives contain sulfur, chlorine, and phosphorus. These additives form layers of sulfides, chlorines, or phosphides that are easily sheared on the metal surface, preventing excessive wear and seizure. However, most additives that perform well with mineral-based oils do not work well with vegetable lubricants [5]. Additionally, substances containing sulfur, chlorine, and phosphorus have been prohibited since they are hazardous to human health and the environment. With the development of nanotribology, increasingly nanoparticles (NPs) are used to overcome the limitations of pure vegetable oil and commercial lube oils, and their unique properties qualify them as friction modifiers (FMs) [31]. Nanoparticle additives in engine oil could help automotive engines use less energy and burn fuel more efficiently by reducing friction and improving the thermal stability of the lubricant [32, 33].

The inclusion of NPs in vegetable oil to improve lubrication properties is the subject of extensive research and development with the goal of developing the ideal biodegradable lubricant. Using a four-ball tribotester, Zulkifli et al., investigated the tribological characteristics of two lubricating oils: paraffin oil and TMP ester made from palm oil combined with $TiO_2$ NPs as an additive. At high loads, TMP ester combined with NPs lowered the coefficient of friction (CoF) by up to 15%. Additionally, NPs lowered the TMP esters' wear scar diameter by developing an additional layer of protection, particularly under low load [34]. Using a ball-on-disc tribometer, Kumar et al. carried out an experimental examination of the tribological performance of canola oil containing copper oxide (CuO) NPs. As per their findings, the coefficient of friction (CoF) and specific wear rate (SWR) was lowered by 61.11% and 64.70% respectively, at the optimal concentration of 0.1 wt% [35]. Kerni et al. studied the impact of Cu and h-BN NPs at various concentrations to examine the friction and wear behavior of epoxidized olive oil on a pin-on-disc tribo-tester. In the boundary lubrication regime, it was discovered that nanoparticle (NP) concentrations of 0.5 wt% exhibit the lowest CoF [36].

The improved friction and wear reduction reported with the inclusion of NPs in lubricating oil is the result of several mechanisms. These mechanisms include modified ball bearings, polishing, mending, and the production of protective films [37–39]. The primary reason for the anti-friction and anti-wear behavior of nanolubricant is the

self-healing mechanism by which nanoparticle tribo-films form on worn surfaces [40, 41]. The various NPs that are used as nano additives are classified as carbon derivatives, metals, metal oxides, nanocomposite materials, rare earth compounds, and sulfides [42]. However, most of the identified nano-additives have active atoms that are either heavy metals, sulfur, or phosphorus, which pose serious environmental risks [43]. In the present work calcium carbonate ($CaCO_3$) NPs were synthesized as a green and eco-friendly modifier that has excellent dispersibility in vegetable oils [44]. The fact that $CaCO_3$ NPs have a favorable low toxicological profile in biological systems implies that they are biocompatible since they don't exhibit any cytotoxicity or genotoxicity—the degree to which a chemical can harm cells and DNA, which is one of the most crucial factors in this choice [45]. To estimate the ranges of application, it is necessary to examine the tribological behavior of the $CaCO_3$ used as a nano-additive. The tribological characteristics of base lubricant oil can be improved by using a low concentration of $CaCO_3$ NPs; Zhang et al. reported an 88.3% reduction in wear volume when PAO containing 1 wt% $CaCO_3$ NPs was used as a lubricant; however, its effect at lower and higher concentrations was not discussed [46]. In the wide concentration range of 0.1 to 5%, Sunqing et al. investigated the tribological behavior of the oil containing $CaCO_3$ NPs. The smallest wear scar diameter and friction coefficient were found when the $CaCO_3$ nanoparticle concentration was between 0.1% and 1.0%. The wear scar diameter and friction coefficient gradually rose when the $CaCO_3$ nanoparticle concentration was raised. These results led to the decision to explore the impact of $CaCO_3$ at lower concentrations using the range of 0.1 to 0.5 wt% of $CaCO_3$ NPs [47].

The criteria for selecting vegetable oil as a lubricating oil in an automatic transmission system, or oil type I, begins with the fact that the selected oil should lubricate the engine after cold starting. An oil with a relatively low viscosity at a low temperature is preferred for this purpose. The lubricants with base oil type I are utilized in fluid couplings, hydraulic torque converters, and automatic transmissions in automobiles. Jojoba and soybean oils are two alternatives from the variety of vegetable oils that can be used for this, as they have properties that are most similar to oil type I, in terms of viscosity. The operating temperature and pressure are the initial factors that determine the best lubricating oil to use in an engine or transmission system. Therefore, it is crucial to consider how oil viscosity may change because of the heat generated during engine operation. Usually, fluid viscosity and temperature have an inverse relationship [48]. El Kinawy et al. explored how jojoba, soybean, sunflower, and castor oils would hold up under severe heating. The viscosity gradient of these oils was assessed after they had been heated for 15 days at 110 °C. Among these oils, jojoba oil has the lowest viscosity gradient [8]. Jojoba (Simmondsia chinensis) oil is extracted from jojoba seeds and offers attractive chemical characteristics. It is regarded as one of the best oils due to its high wax content. It is composed of almost 98% pure waxes, which include mainly wax esters, a few free fatty acids, alcohols, and hydrocarbons. Moreover, flavonoids, phenolic and cyanogenic chemicals, sterols, and vitamins with minimal triglyceride esters are also found [49]. Jojoba oil, as a liquid wax with its fatty acid composition and free fatty acid concentration, is a unique vegetable oil. It is a vegetable oil that is abundant enough to meet industrial lubrication demands [50]. The high lubricity and stability of jojoba oil in the working temperature range of 40 to 100 °C make it a very promising candidate

to study its lubricating properties. Furthermore, it is a non-drying oil that exhibits high resistance to oxidation, has a long shelf life without becoming rancid and contains straight-chain unsaturated double bonds [51]. In arid and semi-arid regions, jojoba is a potential seed oil crop of economic significance. Jojoba bush is an important industrial plant for the rehabilitation of marginal land and the sustainable development of arid and semi-arid regions. As the jojoba plant can thrive in any type of soil and withstand salinity and drought conditions, large-scale cultivation of the plant may be beneficial. This crop is economically significant and could restore the flora and fauna of the land, improve the soil, and stop the process of desertification [52]. With these findings from the literature survey, pure jojoba oil without any chemical modification was chosen as the best choice for the present research work.

A few recent tribological studies with different instrumental setups involving jojoba oil as the base oil and various modifications in the form of added NPs are worth mentioning. A blend of modified jojoba oil and mineral oil transesterified in the presence of graphene NPs was reported to improve tribological performance in a four-ball tribometer test rig and pin-on-disc tribometer [10, 53]. The addition of NPs like $Al_2O_3$ and $TiO_2$ to jojoba oil exhibits improved friction and wear performance [54, 55]. However, there is a lack of studies in the literature that evaluate the anti-wear (AW) and extreme pressure (EP) properties of jojoba oil blended with $CaCO_3$ NPs. The inclusion of $CaCO_3$ nanoparticles will have a significant role in improving the anti-wear and extreme pressure properties of jojoba oil. In this study, we assess the feasibility of using bio-sourced alternative nanolubricants for replacing conventional lubricants that are depleting. Thus, the objective of this research is to experimentally evaluate the anti-wear (AW) and extreme pressure (EP) properties of a nanolubricant derived from jojoba oil and $CaCO_3$ NPs. The lubricating approach discussed in this study is useful for reducing friction and wear in sliding contact applications as well as applications subjected to high loads or shocks, such as turbines, gears, and ball and roller bearings.

## Methods

### Synthesis of NPs and characterization

The nano-regime $CaCO_3$ NPs were synthesized by adopting the novel hydrothermal synthesis route. AR grade calcium nitrate tetrahydrate ($Ca(NO_3)_2\ 4H_2O$) procured from Sigma-Aldrich was dissolved in 50 ml of distilled water. The resultant solution was dropwise added to Ethylenediamine ($C_2H_4(NH_2)_2$) under vigorous stirring. This solution was mixed with Hydrazine ($N_2H_4$) dissolved in 50 ml of distilled water. Finally, the reagents were transferred to an autoclave with a 500 ml capacity, and the reaction was carried out at 140 °C for 24 h before being cooled gradually to room temperature. To remove impurities, the precipitate was centrifuged and washed several times with distilled water and ethanol. The product was finally dried at 80 °C for 10 h. As a result, the received precursors were heated to produce nano-regime crystallites, which became the starting point for all subsequent characterization. Table 1 shows the details of chemicals used for the synthesis of NPs.

The phase composition of the produced powder sample was determined using X-ray Diffraction (XRD). The XRD patterns were acquired in the 20–60° range, with a virtual step-scan of 0.005 and a counting time of 100 s on a Bruker X-ray diffractometer

**Table 1** Chemical description table

| Chemical name | Chemical formula | Source | Purity |
|---|---|---|---|
| Calcium nitrate tetrahydrate | $Ca(NO_3)_2\,4H_2O$ | Sigma-Aldrich | 99.9% |
| Ethylenediamine | $C_2H_4(NH_2)_2$ | Sigma-Aldrich | 99.9% |
| Hydrazine | $N_2H_4$ | Sigma-Aldrich | 99.9% |

(Model D2 PHASER) with $CuK_\alpha$ radiation ($\lambda = 1.5405$, 40 kV and 40 mA). The data collected was used to examine the nano-regime crystallites. The phase identification was performed and compared to the standard JCPDS diffraction patterns 00–005-0586 for $CaCO_3$ calcite [56]. The relative crystalline phase composition was estimated by comparing the areas of the 100% peaks after background subtraction. The compositional assertion and the complexation accuracy confirmation of the prepared powder samples were carried out by the energy dispersive X-ray analysis (EDX) technique. Scanning electron microscope (SEM) measurements were carried out on TESCAN (Model MIRA3 LMH). The surface morphology of the prepared NPs was studied using a SEM by coating the sample with gold. The IR spectral (FTIR) measurements were carried out in the range of 400–4000 $cm^{-1}$ wavenumber on a Shimadzu (Model IRAffinity-1) instrument. The experimental density ($\rho_{exp}$) of NPs was determined by weighing in air and a reference medium while keeping all other variables at ambient conditions. The formulas and procedural details involved are discussed in detail elsewhere [57]. The dynamic light scattering (DLS) based hydrodynamic size and surface charge (zeta potential) of nanoparticle dispersions were characterized using the ZetaSizer Nano ZS (Malvern Instruments Inc., UK). The ISO 13099 standards were used to evaluate nanoparticle dispersion zeta potential values. The samples were filled into the dip cell and loaded into the Zetasizer. The signals were collected, and the data was analyzed using Zetasizer software. Surface zeta potential was measured as per the protocol set by Malvern Instruments using the surface zeta potential cell (zen1020, Malvern Instruments) and the zeta potential transfer standard (DTS1235, Malvern Instruments) as tracer particles (zeta potential $= -42.0$ mV $\pm 4.2$ mV, pH $= 9.2$) [58].

### Sample preparation

Jojoba oil was procured from Kelkar Foods & Fragrance, Pune, India, and used as a base oil without further purification. There are various methods developed for enhancing the stability of nanofluids. The addition of dispersant, stirring, and sonication are noteworthy methods [59]. Considering the toxicity and environmental risks of using surfactants, the present work includes stirring and sonication for the effective dispersion of NPs in the base oil [60]. The nanolubricant samples with weight fractions of 0.1%, 0.2%, 0.3%, 0.4%, and 0.5% (J01, J02, J03, J04, and J05) of the $CaCO_3$ NPs were prepared by a two-step method [59]. To obtain stable and homogenous nanolubricant samples, stirring was performed for 2 h. The high-speed stirred samples were subjected to sonication (Chrom Tech, Inc.) at a frequency of 57 kHz for 1 h at room temperature. After sonication, the $CaCO_3$ NPs show good dispersion stability, improving the dispersion process by physically dissolving the aggregates [56].

### Nanolubricant properties

A study of thermo-physical properties of nanolubricants can provide valuable information about the inclusion of NPs in the nanolubricant formulations [61, 62]. The thermo-physical properties of the nanolubricant oil, namely kinematic viscosity, flash point, and pour point, were assessed. Viscosity, flash point, and pour point measurements were carried out according to the D445-06 standard, ASTM D93 standard, and ASTM D97 standard, respectively [63]. Nanofluid stability refers to the assessment of the dispersion of NPs in a base oil. Dynamic light scattering (DLS) was used in this study to assess the stability, sedimentation, and agglomeration states of nanofluids [64, 65]. The prepared nanofluids were placed in glass containers. The stability of the nanofluids was measured by collecting samples from the top and bottom of the container in its stationary state after 10, 20, and 30 days. These samples were subjected to DLS testing.

One of the limiting factors in lubricant usage is the reaction of oil's chemical entities with oxygen, which results in oxidation. This oxidation leads to the gelation of oil, making it unpumpable, forming an acidic amalgam, reducing heat transfer abilities, and losing the purpose of lubrication. FT-IR analysis provides supportive, if not conclusive, evidence about the oxidation of oil [66, 67]. The modification in the oxidation state of the base oil with the inclusion of $CaCO_3$ NPs was studied using FT-IR analysis, which was performed using an IRAffinity-1S spectrophotometer with a resolution of 4 $cm^{-1}$. The oil samples collected after conducting tribology tests were subjected to FT-IR characterization.

### Tribological tests

The tribological performance of jojoba oil samples with and without the addition of calcium carbonate ($CaCO_3$) NPs, i.e., coefficient of friction (CoF) and wear scar diameter (WSD), was investigated experimentally using a four-ball testing machine. The American Society for Testing and Materials (ASTM) standards were used as the basis for all the trials. The test was conducted on a DUCOM TR-30L four-ball tester. Figure 1 shows the four-ball tribometer test rig used for this investigation with a schematic representation of the four-ball tester. The test balls used in this experiment were made of AISI 52,100 steel with a diameter of 12.7 mm and a Rockwell hardness of 64 HRC. Acetone was used to clean the test balls. The equipment was assembled with clean balls, and the oil cup was filled with 10 ml of oil. All tests were conducted at a constant rotating speed and load with a varying weight percent concentration of NPs in the jojoba oil. The ASTM D4172 guidelines were used to evaluate the relative wear preventive properties of lubricating fluids in sliding contact, also known as anti-wear (AW) properties. It represents two surfaces that slide against each other. A total of six tests were carried out, one on each sample. Each test was performed three times under the same experimental conditions, and the CoF and WSD reported here are the arithmetic means of the measured values from those three tests. To report the variation in the result values, the standard deviation was calculated. The test was run for 3600 s at a constant temperature of 75 °C. The four-ball tester has a fourth ball that is held in a spinning spindle in addition to three balls that are kept stationary in a ball pot. Four balls were subjected to a 40 kgf (392.27 N) force at a spindle speed of 1200 rpm. The wear caused on the three stationary balls is

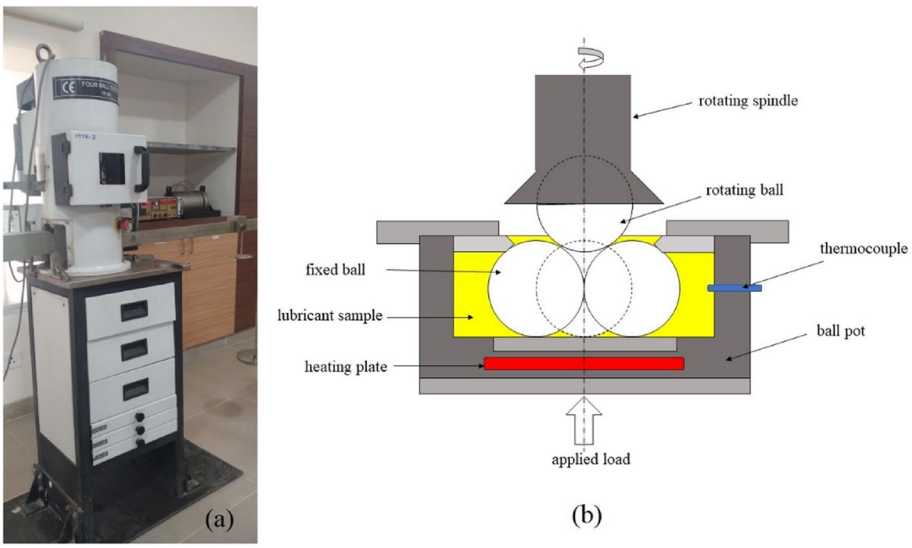


**Fig. 1** **a** Four-ball tribometer test rig used for this investigation and **b** schematic representation of the four-ball tester

measured and reported as the wear scar diameter (WSD). The formula below is used to compute CoF at ball contact [68].

$$\mu = \frac{2.23 \times \text{Frictional torque (kg.cm)}}{\text{Load (kg)}} \tag{1}$$

The four-ball tester consists of a load cell and arm attached to the ball pot, and a controller displays the frictional torque (FT).

The samples were evaluated for extreme pressure (EP) properties in accordance with ASTM D2783. The test simulates applications that may be subjected to high loads or shocks, such as turbines, gears, and ball and roller bearings. The fourth ball in the ball pot was rotated at 1760 rpm for 10 s while the other three balls remained still in the ball pot. As soon as the balls were welded or smoke began to emanate from the ball pot, the tests were stopped. Ten tests were conducted in succession for each sample with increasing loads until the balls weld or smoke is seen from the ball pot. The initial run was performed at a starting load of 32 kgf (313.81 N), and subsequent runs were performed using the standard method at progressively greater loads prescribed as per the test standard until the fluid film broke and direct surface contact occurred (welding of balls). The wear scar diameter (WSD) on the stationary balls was measured using a calibrated optical microscope and plotted versus the applied load.

The Hertz line, compensation line, Hertz diameter (Dh), last nonseizure load (LNSL), initial seizure load (ISL) load wear index (LWI), and weld point load (WPL) were obtained and analyzed as per the test standard. The average diameter of an indentation formed by the deformation of the ball under static conditions is known as the Hertz scar diameter (dh). Plotting the Hertz scar diameter versus load yielded the Hertz line. The compensation scar diameter is defined as the typical diameter of the wear scar on the fixed balls left by the rotating ball when a load is applied and lubrication is present, but without generating seizure or welding. The compensation line was produced from a

comparison of the compensation scar diameters vs applied load. The last load at which the measured scar diameter is not more than 5% over the compensation line at the load is referred to as the last non-seizure load (LNSL). Table 2 shows the experimental conditions of the four-ball tribometer as per the ASTM D4172 and ASTM D2783.

Using an optical vision measuring machine (VMM; Sipcon-SVI-IMG-3D), wear scar diameters (WSD) were measured. The MSU-3DPro software was used to visualize and measure the wear scar on a computer with an accuracy of 0.001 mm. To identify the components on wear scar surfaces, energy dispersive spectrometry (EDS) was employed. An uncertainty analysis was performed to identify the uncertainties in a measured variable caused by environmental, manual, and instrumental errors. Using Eqs. (2) and (3), uncertainty was calculated for a single independent variable and several independent variables where R is the result of the experiment [69].

$$\delta R_{Xi} = \frac{\partial R}{\partial Xi}\delta X_i \tag{2}$$

$$\delta R = \left\{ \sum_{i=1}^{N} \left( \frac{\partial R}{\partial Xi}\delta X_i \right)^2 \right\}^{\frac{1}{2}} \tag{3}$$

The estimated value of uncertainty (±) for CoF is 1.1%

## Results and discussion

As per the XRD analysis, the identified peaks were assigned to pure $CaCO_3$ (calcite) as indicated in Fig. 2. The astute observation of sample morphology (SEM) is presented in Fig. 3, revealing clumped and agglomerated features with dense, homogeneous microstructure. Calcination during synthesis resulted in grain growth transforming into well-faceted solid bodies. The identified elements as per the EDX analysis are shown in Fig. 4, revealing the accurate percentage of each element in the composition free from any impurity. The bulk density of the prepared sample varied by around 10% below that of the corresponding X-ray density ($\rho_{X\text{-}ray}$) due to the unavoidable generation of pores during the synthesis process [70]. The particle size was found to be 22 nm with a specific surface area of 52.5 $m^2/g$. The crystalline nature and nano-regime particle size are indicated by the Scherrer perspective for calculating crystallite size from zenith broadening. All the zenith peaks in the diffractograms were considered for the determination of the

**Table 2** Test conditions of four-ball tribometer

| Parameter | Unit/specification | ASTM D4172 | ASTM D2783 |
|---|---|---|---|
| Ball material | | AISI 52,100 STEEL | AISI 52,100 STEEL |
| Ball diameter | mm | 12.7 | 12.7 |
| Ball hardness | HRC | 64–66 | 64–66 |
| Ball surface roughness (Ra) | mm | 0.022 | 0.022 |
| Load | kgf | 40 | 32 to 250 |
| Spindle speed | rpm | 1200 ± 60 | 1760 ± 60 |
| Test duration | Second | 3600 | 10 |
| Test temperature | °C | 75 ± 2 | 32 ± 2 |

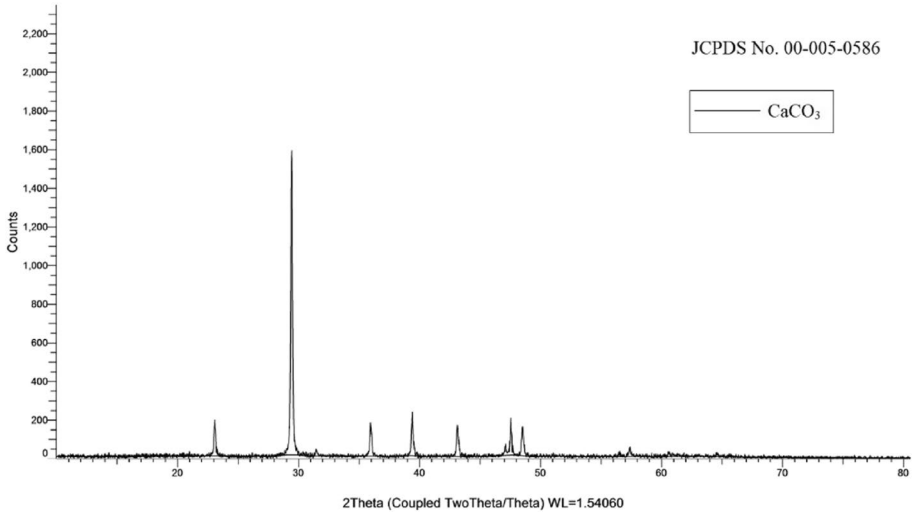


**Fig. 2** XRD of $CaCO_3$ NPs

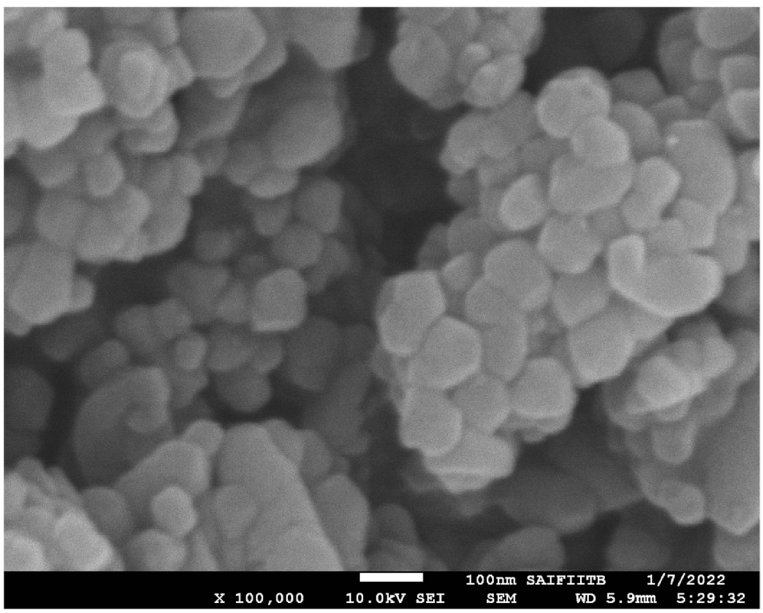


**Fig. 3** SEM of $CaCO_3$ NPs

full horizontal spread of Θ value at the exact half of the intensity. It confirmed that synthesized particles were nanosized. Agglomerated NPs with a nearly spherical shape were evidenced in the representative SEM images.

### Thermo-physical properties

Thermo-physical properties of nanolubricants shed light on the important factors affecting their overall performance [71]. The thermo-physical properties of base oil get modified with the inclusion of NPs, which can lead to better lubricant performance. The higher flash and fire points of jojoba oil as compared to other vegetable oils provide

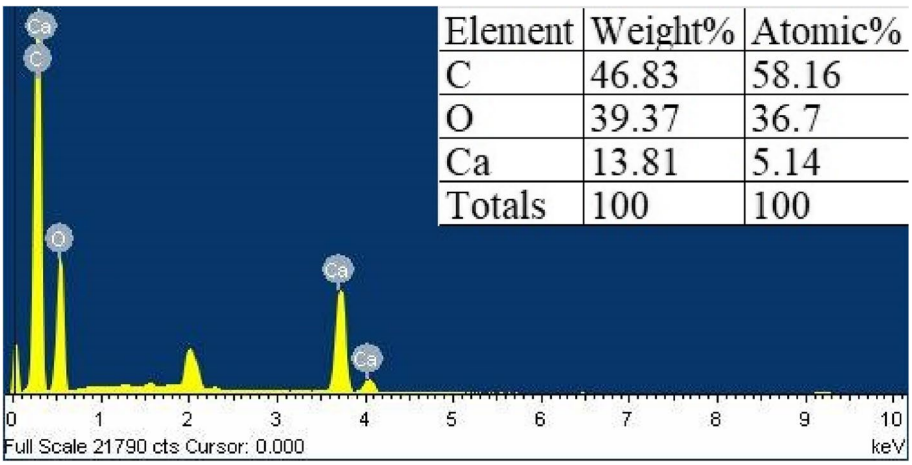


| Element | Weight% | Atomic% |
|---|---|---|
| C | 46.83 | 58.16 |
| O | 39.37 | 36.7 |
| Ca | 13.81 | 5.14 |
| Totals | 100 | 100 |

**Fig. 4** Energy dispersive (EDX) of $CaCO_3$ NPs

**Table 3** Thermo-physical properties of jojoba oil

| Properties | Unit/specification | Jojoba oil | ASTM standard |
|---|---|---|---|
| Kinematic viscosity | cSt at 40 °C<br>at 100 °C | 24.75<br>6.43 | D789 |
| Viscosity index | | 233 | D2270 |
| Flash point | °C | 224 | D93 |
| Pour point | °C | 8 | D97 |

assurance about its safe inclusion as a lubricant. In the present case, it was observed that increasing the concentration of $CaCO_3$ NPs resulted in a slight rise in the flash point. It changed from 224 °C for the base oil to 231 °C for the highest concentration (0.5 wt%). This change in flash point indicates that there are no additional safety requirements for using nanolubricant oils [72]. The pour point rose for the first three concentrations up to 10 °C and decreased to 6 °C for a 0.4 wt% concentration. The presence of $CaCO_3$ in the base oil altered the consistency of distribution. The Thermo-physical properties of pure jojoba oil are listed in Table 3.

The viscosity is one of the figures of merit for a lubricant, as it modifies the film thickness and the wear rate of the sliding surfaces. While higher values of viscosity are an indication of the deterioration of used oil caused by contamination or oxidation, decreased viscosity is an indication of dilution. The kinematic viscosity of prepared nanolubricant samples was measured at 40 °C and 100 °C. The kinematic viscosity values were observed to be lower at 100 °C as compared to 40 °C (Table 4). This observation could be correlated with the fact that there is a reduction in oil layer forces at higher temperatures. In general, there was an increasing trend in viscosity values at both 40 °C and 100 °C as the concentration of $CaCO_3$ in oil increased. When $CaCO_3$ NPs are added to the oil, the viscosity index rises to 237, indicating that the viscosity of the nanolubricant varies less with temperature than base oils. These results are similar to contemporary nanolubricant systems [73–75]. This behavior is related to the catalytic properties of NPs. A slight increase in the viscosity values of the nanolubricant oils is desirable as it leads to

**Table 4** Kinematic viscosity and viscosity index of samples

| Sample | Kinematic viscosity at 40 °C (cSt) | Kinematic viscosity at 100 °C (cSt) | Viscosity index |
|---|---|---|---|
| J00 | 24.75 | 6.43 | 233 |
| J01 | 24.82 | 6.48 | 235 |
| J02 | 24.95 | 6.51 | 235 |
| J03 | 25.02 | 6.55 | 237 |
| J04 | 25.12 | 6.56 | 236 |
| J05 | 25.13 | 6.56 | 236 |

improvements in the lubricating properties and the prevention of rapid wear. In the present formulations, the viscosity of nanofluids was found to decrease with an increase in temperature and increase with an increase in particle concentration. Weakening of the intermolecular forces of lubricant with a rise in temperature is enhanced with nanoparticle inclusion in organic oils. The formation of a lubricating film between contacting surfaces was positively influenced by the increase in nanoparticle concentration. The fact that the heat dissipation was also enhanced was attributed to the viscous nature of the fluid, which was able to withstand a higher temperature as compared to the base oil, which disintegrated easily with the rise in temperature. The addition of nanoparticles tends to alter the base fluid's rheological behavior [76–78]. In the present case, for 0.4 and 0.5 wt% concentrations at lower shear rates, non-Newtonian behavior is observed. Moreover, at higher shear rates, the nanolubricants behave as Newtonian fluids in the temperature range of 40 °C and 100 °C for all concentrations.

The zeta potential is a measurement of the difference in potential between the NP's stern layer and the base oil. The Zeta Sizer was used to measure the value of zeta potential. The zeta potential of a nanofluid reveals its stability; the higher the zeta potential, the more stable the nanofluid. The zeta potential values in the present case varied in the range from − 47.13 to − 51.46 mV, revealing the stability of nanofluids [79]. The nanofluid samples at higher concentrations scattered more light, and hence, the intensity of the scattered light decreased (Fig. 5). For 30 days, the highest concentration caused the most sedimentation. The intensity results showed that samples with a concentration of 0.3 were stable after 20 days. The sedimentation was found to be higher for the 0.4 and 0.5 wt% concentrations after 30 days.

The nanolubricant concentrations under consideration revealed a change in the FTIR peaks. This probably indicated that the nano-additives have a synergistic chemical reaction with jojoba oil. The suspension of the NPs has been beneficial for reducing friction and wear volume [68]. The bands corresponding to the fatty acid group and ester group were beneficial from a tribological study point of view. FT-IR absorption bands corresponding to stretching and bending of the olefinic (=CH) group were observed at 3003 and 721 $cm^{-1}$ (Fig. 6). Other stretching absorption bands were found at 1651, 1737, 1244, and 1170 $cm^{-1}$, which correspond to the (C=C) bond, (C=O), and (C–O) of the ester group, respectively. The bands appearing at 2922 and 2852 $cm^{-1}$ were assigned to $CH_3$ and $CH_2$ groups, respectively. The oxidation state of organic esters led to the absorption band in the regions 1660–1710 $cm^{-1}$ and 3540–3560 $cm^{-1}$ [80]. A small alteration occurs in the cis CH band at 3003 $cm^{-1}$ as an indication of the oxidative process. The

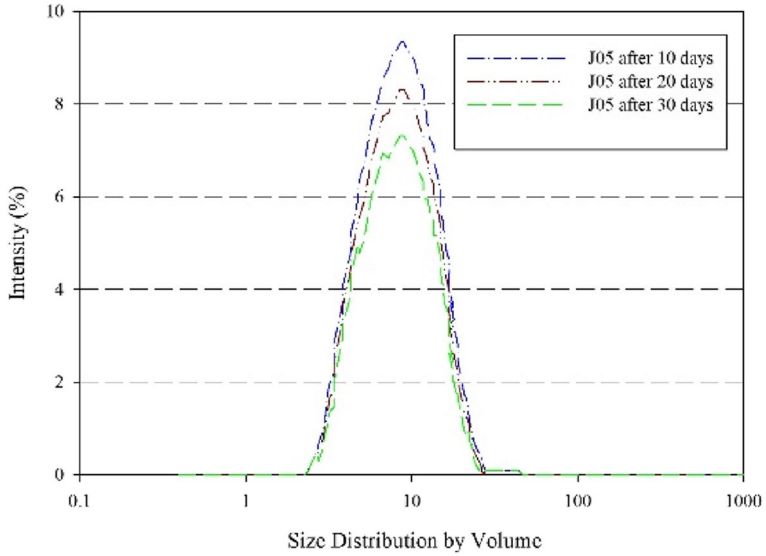


**Fig. 5** DLS size distribution of J05 after 10, 20, and 30 days

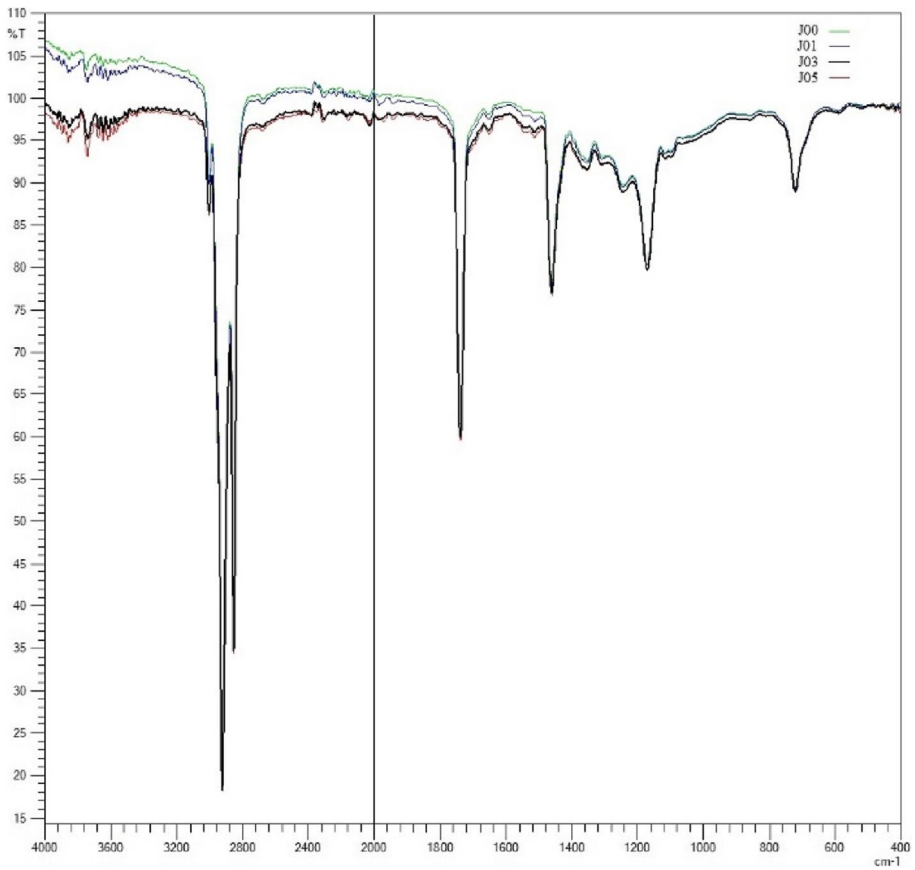


**Fig. 6** FT-IR spectrum of oil samples

intensity of these absorption bands was slightly modified with the increase in the nanoparticle concentration. The results presented here are in agreement with similar studies [81]. The oxidation in nanolubricants proceeds through multiple steps. Starting with the generation of free radicals, it proceeds to combine with oxygen to produce peroxide radicals. Finally, these radicals combine with other lubricant components to form a stable molecule. The reduction in absorbance value of peaks related to the C=O, C–H, $CH_2$, and $CH_3$ functional groups shows the anti-oxidation role of nanoparticles exhibiting good stability.

#### Anti-wear (AW) and Extreme-pressure (EP) properties

Throughout the experiment, the CoF was measured every 30 s; the four-ball test's fluctuation in CoF with time is depicted in Fig. 7. The CoF, averaged from 120 original data points for every sample, is plotted in Fig. 8. All lubricating oils containing $CaCO_3$ NPs have lower friction coefficient values than lubricating oil in its purest form. Sample J03 has the lowest average CoF of 0.0938, while sample J00 has the highest average CoF of 0.1318. There is a slight increase in CoF friction for J04 and J05 as compared to the lowest value of CoF for J03, where J05 represents the highest concentration of 0.5 wt%. $CaCO_3$ nanoparticles at 0.1 wt% failed to cover the entire contact surface, resulting in a higher CoF than at 0.3 wt%. Whereas a higher $CaCO_3$ percentage in the nanolubricant caused some $CaCO_3$ nanoparticles to agglomerate, resulting in larger secondary particle sizes. This would lead to increased friction and wear, which would increase the coefficient of friction.

The WSD of the three lower balls in the four-ball test serves as a reflection of the lubricant's anti-wear property, and a smaller WSD denotes a higher level of wear resistance. The WSD of six samples measured using optical vision is shown in Fig. 8. It was found that sample J00, which contained the purest lubricating oil, had a WSD value of 561 μm. The WSD is minimized by adding $CaCO_3$ NPs to the base oil. WSD reduces

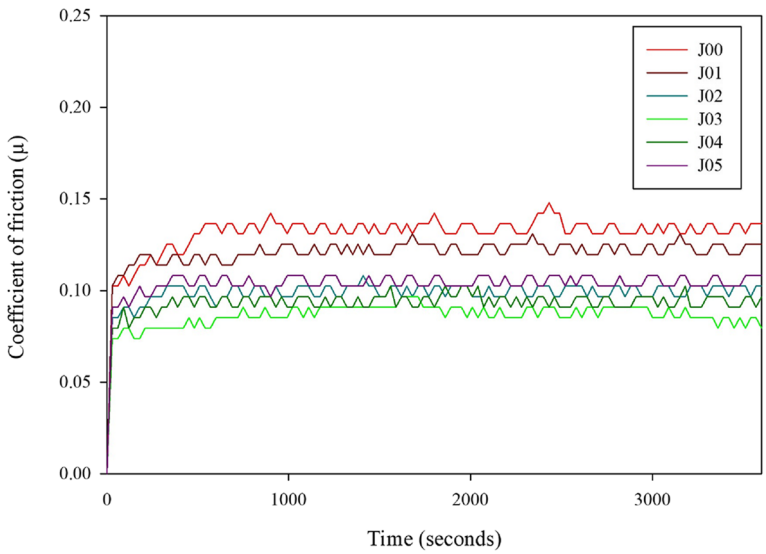


**Fig. 7** Coefficient of friction vs. time for concentrations of $CaCO_3$ NPs in jojoba oil

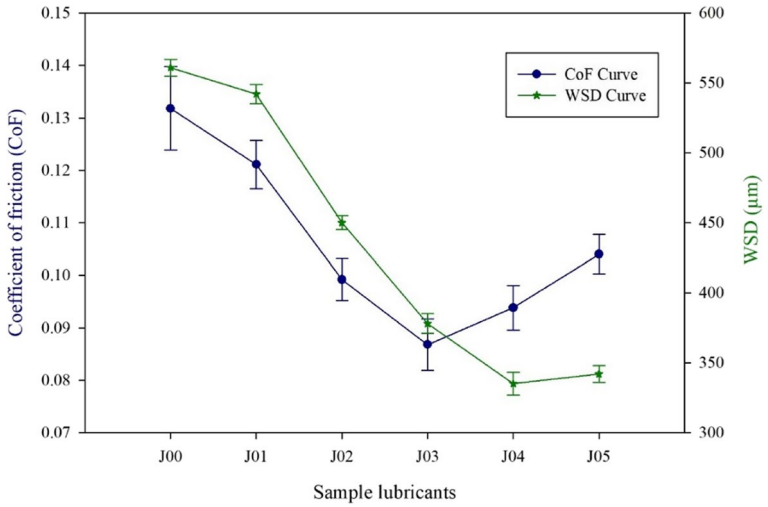


**Fig. 8** Friction coefficient and wear scar diameter as a function of additive concentration

as NP concentration rises until sample J04. Base oil has the lowest WSD with an NP concentration of 0.4 wt%. The sample with the highest concentration of NPs, J05, sees a small increase in WSD.

The purpose of the ASTM D2783 test is to determine the load-carrying capacity of oil samples under extreme pressure (EP). The extreme pressure region is the zone beyond the LNSL, whereas the anti-wear region is the zone before the LNSL. Initial seizure load (ISL) is the load at which there is a brief breakdown of the lubricating film when a load is applied. This breakdown can be identified by a sudden increase in the reported scar diameter and a quick deflection of the friction-measuring device. The lowest applied load at which the revolving ball welds to the three fixed balls is known as the weld point load (WPL). The overall EP behavior is exhibited by the load-wear index (LWI) or load-carrying capability of a lubricant.

Figure 9 shows the applied load against WSD at extreme pressure conditions, with and without the addition of NPs. The WSD was reduced for all NP concentrations in jojoba oil starting with the LNSL. When compared to the position of the curve for pure base oil, the curves of the $CaCO_3$ nanoparticle-enriched oils (J04 and J05) shifted to the lower side. As a result, the addition of NPs enhanced the LWI for these samples. The observed LWI value is proportional to the concentration of NPs till sample J04 (Table 5). The maximum value of LWI is observed for J04, although the value of LWI for J05 is very close to that. The LNSL showed no significant difference between a pure oil and oil-containing low concentrations of NPs (J01, J02, and J03); however, the LNSL value for J04 and J05 increased from 490 to 618N compared to the low concentration samples, and similar behavior was observed for the ISL and WPL, indicating improved EP behavior. The suspension containing 0.4 wt% of NPs displayed the best tribological performance, confirming the ability of $CaCO_3$ NPs to resist wear under high-loading conditions. Figure 10 shows the WSD at the maximum load before the weld point for all the samples (J00 to J05).

The worn-out balls obtained after tribological tests were subjected to EDS analysis to find out if there were any $CaCO_3$ NPs present on the worn-out surface of the ball.

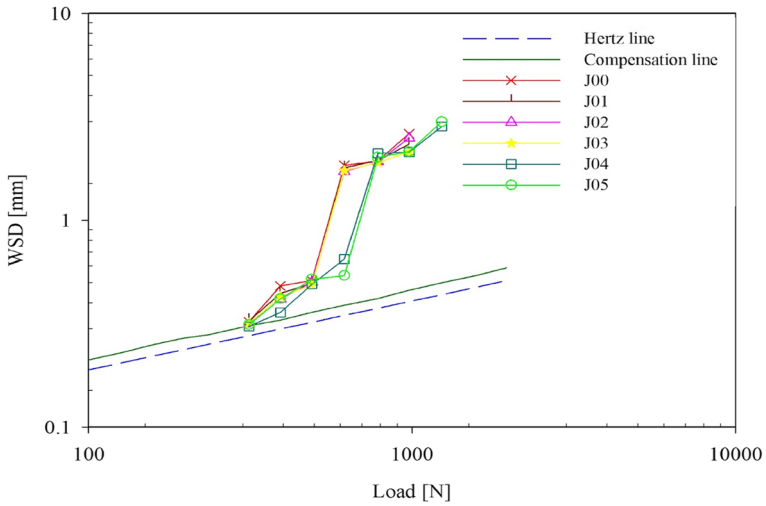


**Fig. 9** Wear scar diameter vs. load curve for various concentrations of $CaCO_3$ NPs in jojoba oil

**Table 5** Extreme pressure properties of sample lubricants

| Lubricant | Last nonseizure load, LNSL (N) | Initial seizure load, ISL (N) | Weld point Load, WPL (N) | Load-wear Index, LWI (N) |
|---|---|---|---|---|
| J00 | 490 | 618 | 1236 | 206.66 |
| J01 | 490 | 618 | 1236 | 214.81 |
| J02 | 490 | 618 | 1236 | 217.99 |
| J03 | 490 | 618 | 1236 | 222.11 |
| J04 | 618 | 784 | 1569 | 253.78 |
| J05 | 618 | 784 | 1569 | 252.80 |

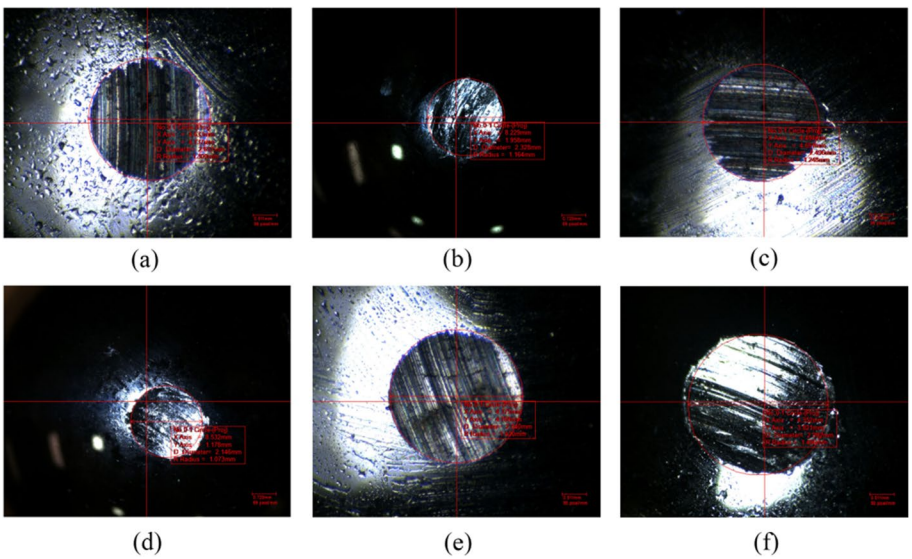


**Fig. 10** WSD at the maximum load before weld point for all the samples, where **a** J00, **b** J01, **c** J02 **d** J03 **e** J04, and **f** J05

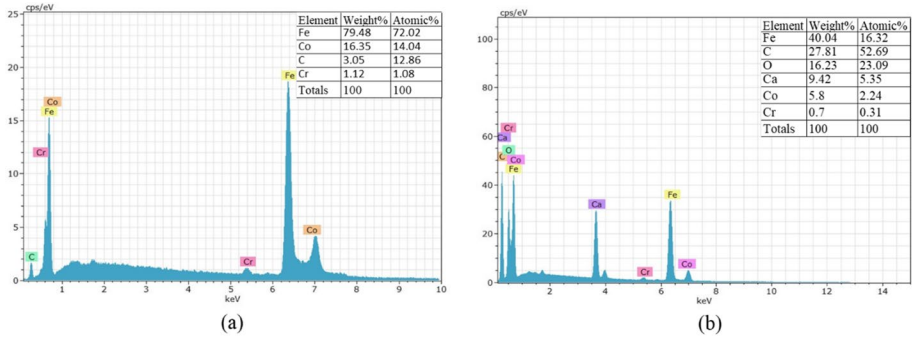


**Fig. 11** Energy dispersive (EDX) of worn-out balls for sample **a** J00 and **b** J04

Reference base oil and a specific concentration of 0.4 wt% NPs EDS images are shown in Fig. 11 a and b respectively. A peak of the elements Ca and O can be seen in the EDS spectra of the worn-out surfaces, indicating the existence of $CaCO_3$ (Fig. 11 b), whereas there are no traces of Ca and O on the worn-out surface of the ball used in pure base oil (Fig. 11 a). Spherical $CaCO_3$ NPs may have micro-ball bearing and friction-reducing effects on the friction surface by filling concave holes, repairing and separating the friction surfaces. The formation of secondary phases of the $CaCO_3$ NPs like CaO and $CO_2$ due to decomposition may be formed when the temperature and pressure reach a certain level. A small trace of $Ca^{2+}$ may also form due to the ionization of $CaCO_3$ NPs. The formation of metal calcium may thus be related to a calcium ion capturing two electrons. These complex tribological chemical reactions on the friction surface form metal calcium and calcium oxide films, which can fill up the worn surface and protect it from wear, which improves the lubrication behavior of the base oil [44, 82].

## Conclusions

Nanolubricant samples of jojoba oil with the $CaCO_3$ NPs prepared by a two-step method demonstrated good dispersion stability. Given the environmental risks, the approach of using no surfactants for nanoparticle stability was found to be effective in the present case. Besides being eco-friendly, the prepared nanolubricants in all the concentrations revealed remarkable anti-wear (AW) and extreme-pressure (EP) properties. The lubricant oil performed optimally in terms of anti-friction at 0.3 wt% of $CaCO_3$ NPs, and the average friction coefficient and the average wear scar diameter of the steel balls decreased by as much as 34.1% and 40.2%, respectively. Whereas the suspension with 0.4 wt% of NPs performed best under extreme pressure conditions, with significant improvements in the last non-seizure load, the initial seizure load, the weld point load, and the load wear index. The anti-wear mechanism is entirely attributed to $CaCO_3$ nanoparticle deposition and the formation of metal calcium and calcium oxide films as a result of tribo-chemical reactions. The study demonstrates the benefit of using $CaCO_3$ NPs and Jojoba oil in the field of tribology. High-performance $CaCO_3$-based nanolubricants appear to be a commercially viable alternative to traditional anti-wear, anti-friction, and extreme-pressure lubricating oils.

**Abbreviations**

| | |
|---|---|
| AISI | American Iron and Steel Institute |
| AR | Analytical research |
| ASTM | American Society for Testing and Materials |
| AW | Anti-wear |
| CoF | Coefficient of friction |
| Dh | Hertz diameter |
| DLS | Dynamic light scattering |
| EDX/EDS | Energy dispersive X-ray analysis |
| EP | Extreme pressure |
| FMs | Friction modifiers |
| FTIR | Fourier transform infrared |
| HRC | Hardness on Rockwell scale C |
| ISL | Initial seizure load |
| J00 | Pure jojoba oil |
| J01 | Nanolubricant samples with weight fractions of 0.1% |
| J02 | Nanolubricant samples with weight fractions of 0.2% |
| J03 | Nanolubricant samples with weight fractions of 0.3% |
| J04 | Nanolubricant samples with weight fractions of 0.4% |
| J05 | Nanolubricant samples with weight fractions of 0.5% |
| JCPDS | Joint Committee on Powder Diffraction Standards |
| LNSL | Last non-seizure load |
| LWI | Load wear index |
| NPs | Nanoparticles |
| SEM | Scanning electron microscope |
| SWR | Specific wear rate |
| TMP | Trimethylolpropane |
| WPL | Weld point load |
| WSD | Wear scar diameter |
| wt % | Weight fractions |
| XRD | X-ray diffraction |

**Acknowledgements**
Not applicable.

**Authors' contributions**
TK conceptualized the study, wrote the original draft, analyzed the data, and reviewed the article. TK and BT conducted the experimentation. AC and JN contributed to the synthesis and characterization of nanoparticles. AA has contributed to developing the methodology, writing, and reviewing the article. The authors have read and approved the final manuscript.

**Funding**
The authors declare that no funds, grants, or other support were received during the preparation of this manuscript.

**Availability of data and materials**
The datasets used and/or analyzed during the current study are available from the corresponding author on reasonable request.

## Declarations

**Competing interests**
The authors declare that they have no competing interests.

Received: 20 February 2023 Accepted: 14 April 2023
Published online: 21 April 2023

**References**

1. Aluyor EO, Ori-jesu M (2009) Biodegradation of mineral oils – a review. Afr J Biotech 8(6):915–920. https://doi.org/10.4314/ajb.v8i6.59986
2. Tamada IS, Lopes PRM, Montagnolli RN, Bidoia ED (2012) Biodegradation and toxicological evaluation of lubricant oils. Braz Arch Biol Technol 55:951–956. https://doi.org/10.1590/S1516-89132012000600020
3. Reeves CJ, Menezes PL, Jen T-C, Lovell MR (2015) The influence of fatty acids on tribological and thermal properties of natural oils as sustainable biolubricants. Tribol Int 90:123–134. https://doi.org/10.1016/j.triboint.2015.04.021
4. Erhan SZ, Sharma BK, Liu Z, Adhvaryu A (2008) Lubricant base stock potential of chemically modified vegetable oils. J Agric Food Chem 56(19):8919–8925. https://doi.org/10.1021/jf801463d
5. Darminesh SP, Sidik NAC, Najafi G, Mamat R, Ken TL, Asako Y (2017) Recent development on biodegradable nanolubricant: a review. Int Commun Heat Mass Transfer 86:159–165. https://doi.org/10.1016/j.icheatmasstransfer.2017.05.022
6. Adhvaryu A, Erhan SZ, Perez JM (2004) Tribological studies of thermally and chemically modified vegetable oils for use as environmentally friendly lubricants. Wear 257(3):359–367. https://doi.org/10.1016/j.wear.2004.01.005

7. Bisht RPS, Sivasankaran GA, Bhatia VK (1993) Additive properties of jojoba oil for lubricating oil formulations. Wear 161(1):193–197. https://doi.org/10.1016/0043-1648(93)90469-3
8. el Kinawy O (2004) Comparison between jojoba oil and other vegetable oils as a substitute to petroleum. Energy Sourc 26(7):639–645. https://doi.org/10.1080/00908310490438623
9. Harry-O'kuru RE, Biresaw G, Gordon S, Xu J (2018) Physical characteristics of tetrahydroxy and acylated derivatives of jojoba liquid wax in lubricant applications. J Anal Methods Chem 2018:7548327. https://doi.org/10.1155/2018/7548327
10. Thirumalai KK, Rameshbabu S (2018) Tribological properties of modified jojoba oil as probable base stoke of engine lubricant. J Mech Sci Technol 32(4):1739–1747
11. Wu X, Zhang X, Yang S, Chen H, Wang D (2000) The study of epoxidized rapeseed oil used as a potential biodegradable lubricant. J Am Oil Chem Soc 77(5):561–563. https://doi.org/10.1007/s11746-000-0089-2
12. Gryglewicz S, Muszyński M, Nowicki J (2013) Enzymatic synthesis of rapeseed oil-based lubricants. Ind Crops Prod 45:25–29. https://doi.org/10.1016/j.indcrop.2012.11.038
13. Arumugam S, Sriram G (2013) Synthesis and characterisation of rapeseed oil bio-lubricant – its effect on wear and frictional behaviour of piston ring–cylinder liner combination. Proc Inst Mech Eng J J Eng Tribol 227(1):3–15. https://doi.org/10.1177/1350650112458398
14. Zulkifli NWM, Kalam MA, Masjuki HH, Shahabuddin M, Yunus R (2013) Wear prevention characteristics of a palm oil-based TMP (trimethylolpropane) ester as an engine lubricant. Energy 54:167–173. https://doi.org/10.1016/j.energy.2013.01.038
15. Sharma UC, Sachan S (2019) Friction and wear behavior of karanja oil derived biolubricant base oil. SN Appl Sci 1(7):668. https://doi.org/10.1007/s42452-019-0706-y
16. Gorla G, Kour SM, Padmaja KV, Karuna MSL, Prasad RBN (2013) Preparation and properties of lubricant base stocks from epoxidized karanja oil and its alkyl esters. Ind Eng Chem Res 52(47):16598–16605. https://doi.org/10.1021/ie4024325
17. Ghosh P, Karmakar G (2014) Evaluation of sunflower oil as a multifunctional lubricating oil additive. Int J Ind Chem 5(1):7. https://doi.org/10.1007/s40090-014-0007-7
18. Jabal MH, Abdulmunem AR, Abd HS (2019) Experimental investigation of tribological characteristics and emissions with nonedible sunflower oil as a biolubricant. J Air Waste Manag Assoc 69(1):109–118. https://doi.org/10.1080/10962247.2018.1523070
19. Hwang H-S, Erhan SZ (2001) Modification of epoxidized soybean oil for lubricant formulations with improved oxidative stability and low pour point. J Am Oil Chem Soc 78(12):1179–1184. https://doi.org/10.1007/s11745-001-0410-0
20. Adhvaryu A, Erhan SZ (2002) Epoxidized soybean oil as a potential source of high-temperature lubricants. Ind Crops Prod 15(3):247–254. https://doi.org/10.1016/S0926-6690(01)00120-0
21. Rudnick LR (ed) (2005). CRC Press, Boca Raton. https://doi.org/10.1201/9781420027181
22 Sankarannair S, Nair AA, Bijo BV, Das HK, Sureshkumar H (2020) Biolubricant from pongamia oil. tribology in materials and manufacturing - wear, friction and lubrication. IntechOpen. https://doi.org/10.5772/intechopen.93477
23. Singh Y, Garg R, Kumar S (2016) Comparative tribological investigation on EN31 with pongamia and jatropha as lubricant additives. Energy Sourc A Recovery Util Environ Effects 38(18):2756–2762. https://doi.org/10.1080/15567036.2015.1105326
24. Jayadas NH, Nair KP (2006) Coconut oil as base oil for industrial lubricants—evaluation and modification of thermal, oxidative and low temperature properties. Tribol Int 39(9):873–878. https://doi.org/10.1016/j.triboint.2005.06.006
25. Sajeeb A, Rajendrakumar PK (2019) Comparative evaluation of lubricant properties of biodegradable blend of coconut and mustard oil. J Clean Prod 240:118255. https://doi.org/10.1016/j.jclepro.2019.118255
26. Sammaiah A, Padmaja KV, Prasad RBN (2014) Synthesis of epoxy jatropha oil and its evaluation for lubricant properties. J Oleo Sci advpub, ess13172. https://doi.org/10.5650/jos.ess13172
27. Shahabuddin M, Masjuki HH, Kalam MA (2013) Experimental investigation into tribological characteristics of biolubricant formulated from jatropha oil. Procedia Eng 56:597–606. https://doi.org/10.1016/j.proeng.2013.03.165
28. Singh AK (2011) Castor oil-based lubricant reduces smoke emission in two-stroke engines. Ind Crops Prod 33(2):287–295. https://doi.org/10.1016/j.indcrop.2010.12.014
29. Hernández-Sierra MT, Aguilera-Camacho LD, Báez-García JE, García-Miranda JS, Moreno KJ (2018) Thermal stability and lubrication properties of biodegradable castor oil on AISI 4140 steel. Metals 8(6):428. https://doi.org/10.3390/met8060428
30. Syahrullail S, Kamitani S, Shakirin A (2013) Performance of vegetable oil as lubricant in extreme pressure condition. Procedia Eng 68:172–177. https://doi.org/10.1016/j.proeng.2013.12.164
31. Chowdary K, Kotia A, Lakshmanan V, Elsheikh AH, Ali MKA (2021) A review of the tribological and thermophysical mechanisms of bio-lubricants based nanomaterials in automotive applications. J Mol Liq 339:116717. https://doi.org/10.1016/j.molliq.2021.116717
32. Ali MKA, Xianjun H, Mai L, Qingping C, Turkson RF, Bicheng C (2016) Improving the tribological characteristics of piston ring assembly in automotive engines using Al2O3 and TiO2 nanomaterials as nano-lubricant additives. Tribol Int 103:540–554. https://doi.org/10.1016/j.triboint.2016.08.011
33. Jiang H, Hou X, Dearn KD, Su D, Kamal Ahmed Ali M (2021) Thermal stability enhancement mechanism of engine oil using hybrid MoS2/h-BN nano-additives with ionic liquid modification. Adv Powder Technol 32(12):4658–4669. https://doi.org/10.1016/j.apt.2021.10.015
34. Zulkifli NWM, Kalam MA, Masjuki HH, Yunus R (2013) Experimental analysis of tribological properties of biolubricant with nanoparticle additive. Procedia Eng 68:152–157. https://doi.org/10.1016/j.proeng.2013.12.161
35. Kumar V, Dhanola A, Garg HC, Kumar G (2020) Improving the tribological performance of canola oil by adding CuO nanoadditives for steel/steel contact. Mater Today Proc 28:1392–1396. https://doi.org/10.1016/j.matpr.2020.04.807
36. Kerni L, Raina A, Haq MIU (2019) Friction and wear performance of olive oil containing nanoparticles in boundary and mixed lubrication regimes. Wear 426–427:819–827. https://doi.org/10.1016/j.wear.2019.01.022
37. Gulzar M, Masjuki HH, Kalam MA, Varman M, Zulkifli NWM, Mufti RA, Zahid R (2016) Tribological performance of nanoparticles as lubricating oil additives. J Nanopart Res 18(8):223. https://doi.org/10.1007/s11051-016-3537-4

38. Dai W, Kheireddin B, Gao H, Liang H (2016) Roles of nanoparticles in oil lubrication. Tribol Int 102:88–98. https://doi.org/10.1016/j.triboint.2016.05.020
39. Kotia A, Chowdary K, Srivastava I, Ghosh SK, Ali MKA (2020) Carbon nanomaterials as friction modifiers in automotive engines: recent progress and perspectives. J Mol Liq 310:113200. https://doi.org/10.1016/j.molliq.2020.113200
40. Ali MKA, Xianjun H, Abdelkareem MAA, Gulzar M, Elsheikh AH (2018) Novel approach of the graphene nanolubricant for energy saving via anti-friction/wear in automobile engines. Tribol Int 124:209–229. https://doi.org/10.1016/j.triboint.2018.04.004
41. Ali MKA, Hou X, Abdelkareem MAA (2020) Anti-wear properties evaluation of frictional sliding interfaces in automobile engines lubricated by copper/graphene nanolubricants. Friction 8(5):905–916. https://doi.org/10.1007/s40544-019-0308-0
42. Kulkarni T, Autee A, Toksha B, Chatterjee A (2022) Data-driven modeling for tribological performance of nanolubricants using artificial neural network. In 2022 IEEE International Conference on Nanoelectronics, Nanophotonics, Nanomaterials, Nanobioscience & Nanotechnology (5NANO) (pp. 1–12). Presented at the 2022 IEEE International Conference on Nanoelectronics, Nanophotonics, Nanomaterials, Nanobioscience & Nanotechnology (5NANO). https://doi.org/10.1109/5NANO53044.2022.9828932
43. Khan I, Saeed K, Khan I (2019) Nanoparticles: properties, applications and toxicities. Arab J Chem 12(7):908–931. https://doi.org/10.1016/j.arabjc.2017.05.011
44. Gu C, Li Q, Gu Z, Zhu G (2008) Study on application of $CeO_2$ and $CaCO_3$ nanoparticles in lubricating oils. J Rare Earths 26(2):163–167. https://doi.org/10.1016/S1002-0721(08)60058-7
45. d'Amora M, Liendo F, Deorsola FA, Bensaid S, Giordani S (2020) Toxicological profile of calcium carbonate nanoparticles for industrial applications. Colloids Surf B Biointerfaces 190:110947. https://doi.org/10.1016/j.colsurfb.2020.110947
46. Zhang M, Wang X, Fu X, Xia Y (2009) Performance and anti-wear mechanism of $CaCO_3$ nanoparticles as a green additive in poly-alpha-olefin. Tribol Int 42(7):1029–1039. https://doi.org/10.1016/j.triboint.2009.02.012
47. Sunqing Q, Junxiu D, Guoxu C (2000) Wear and friction behaviour of $CaCO_3$ nanoparticles used as additives in lubricating oils. Lubr Sci 12(2):205–212. https://doi.org/10.1002/ls.3010120207
48 Nadeem S, Abbas N, Nadeem S, Abbas N (2019) Effects of MHD on modified nanofluid model with variable viscosity in a porous medium. Nanofluid flow in porous media. IntechOpen. https://doi.org/10.5772/intechopen.84266
49 Gad HA, Roberts A, Hamzi SH, Gad HA, Touiss I, Altyar AE, Ashour ML (2021) Jojoba oil: an updated comprehensive review on chemistry, pharmaceutical uses, and toxicity. Polymers 13(11):1711. https://doi.org/10.3390/polym13111711
50. Ghannam MT, Selim MYE (2021) The flow behavior of raw Jojoba oil in comparison with some traditional lube oils. Ind Crops Prod 161:113164. https://doi.org/10.1016/j.indcrop.2020.113164
51. Abdel-Hameed HS, El-Saeed SM, Ahmed NS, Nassar AM, El-Kafrawy AF, Hashem AI (2022) Chemical transformation of jojoba oil and soybean oil and study of their uses as bio-lubricants. Ind Crops Prod 187:115256. https://doi.org/10.1016/j.indcrop.2022.115256
52 Bala R (2021) Jojoba - the gold of desert. Deserts and desertification. IntechOpen. https://doi.org/10.5772/intechopen.99872
53. Thirumalai Kannan K, RameshBabu S (2017) Tribological behavior of modified jojoba oil with graphene nanoparticle as additive in SAE20W40 oil using pin on disc tribometer. Energ Sourc A Recovery Util Environ Eff 39(17):1842–1848. https://doi.org/10.1080/15567036.2017.1376006
54. Suthar K, Singh Y, Surana AR, Rajubhai VH, Sharma A (2020) Experimental evaluation of the friction and wear of jojoba oil with aluminium oxide (Al2O3) nanoparticles as an additive. Mater Today Proc 25:699–703. https://doi.org/10.1016/j.matpr.2019.08.150
55. Zaid M, Kumar A, Singh Y (2021) Lubricity improvement of the raw jojoba oil with TiO2 nanoparticles as an additives at different loads applied. Mater Today Proc 46:3165–3168. https://doi.org/10.1016/j.matpr.2020.07.437
56. Kawashima S, Seo J-WT, Corr D, Hersam MC, Shah SP (2014) Dispersion of $CaCO_3$ nanoparticles by sonication and surfactant treatment for application in fly ash–cement systems. Mater Struct 47(6):1011–1023. https://doi.org/10.1617/s11527-013-0110-9
57. Shirsath SE, Toksha BG, Jadhav KM (2009) Structural and magnetic properties of In3+ substituted $NiFe_2O_4$. Mater Chem Phys 117(1):163–168. https://doi.org/10.1016/j.matchemphys.2009.05.027
58. ISO 13099–1:2012. (2012). Colloidal systems — methods for zeta-potential determination — part 1: electroacoustic and electrokinetic phenomena. Retrieved from https://www.iso.org/standard/52807.html
59. Ali ARI, Salam B (2020) A review on nanofluid: preparation, stability, thermophysical properties, heat transfer characteristics and application. SN Appl Sci 2(10):1636. https://doi.org/10.1007/s42452-020-03427-1
60. Badmus SO, Amusa HK, Oyehan TA, Saleh TA (2021) Environmental risks and toxicity of surfactants: overview of analysis, assessment, and remediation techniques. Environ Sci Pollut Res 28(44):62085–62104. https://doi.org/10.1007/s11356-021-16483-w
61. Sadiq IO, Sharif S, Suhaimi MA, Yusof NM, Kim D-W, Park K-H (2018) Enhancement of thermo-physical and lubricating properties of SiC nanolubricants for machining operation. Procedia Manuf 17:166–173. https://doi.org/10.1016/j.promfg.2018.10.032
62. Ali MKA, Xianjun H, Turkson RF, Peng Z, Chen X (2016) Enhancing the thermophysical properties and tribological behaviour of engine oils using nano-lubricant additives. RSC Adv 6(81):77913–77924. https://doi.org/10.1039/C6RA10543B
63. Ranjbarzadeh R, Chaabane R (2021) Experimental study of thermal properties and dynamic viscosity of graphene oxide/oil nano-lubricant. Energies 14(10):2886. https://doi.org/10.3390/en14102886
64. Carvalho PM, Felício MR, Santos NC, Gonçalves S, Domingues MM (2018) Application of light scattering techniques to nanoparticle characterization and development. Front Chem 6:237. https://doi.org/10.3389/fchem.2018.00237
65. Cinar G, Solomun JI, Mapfumo P, Traeger A, Nischang I (2022) Nanoparticle sizing in the field of nanomedicine: power of an analytical ultracentrifuge. Anal Chim Acta 1205:339741. https://doi.org/10.1016/j.aca.2022.339741

66. Singh Y, Rahim EA, Singh NK, Sharma A, Singla A, Palamanit A (2022) Friction and wear characteristics of chemically modified mahua (madhuca indica) oil based lubricant with $SiO_2$ nanoparticles as additives. Wear 508–509:204463. https://doi.org/10.1016/j.wear.2022.204463
67. Fotovvat B, Behzadnasab M, Mirabedini SM, Mohammadloo HE (2022) Anti-corrosion performance and mechanical properties of epoxy coatings containing microcapsules filled with linseed oil and modified ceria nanoparticles. Colloids Surf A Physicochem Eng Asp 648:129157. https://doi.org/10.1016/j.colsurfa.2022.129157
68. Nagarajan T, Khalid M, Sridewi N, Jagadish P, Shahabuddin S, Muthoosamy K, Walvekar R (2022) Tribological, oxidation and thermal conductivity studies of microwave synthesised molybdenum disulfide (MoS2) nanoparticles as nano-additives in diesel based engine oil. Sci Rep 12(1):14108. https://doi.org/10.1038/s41598-022-16026-4
69. Moffat RJ (1988) Describing the uncertainties in experimental results. Exp Thermal Fluid Sci 1(1):3–17. https://doi.org/10.1016/0894-1777(88)90043-X
70. Sukumar M, John Kennedy L, Judith Vijaya J, Al-Najar B, Bououdina M (2018) Facile microwave assisted combustion synthesis, structural, optical and magnetic properties of La2−xSrxCuO4 ($0 \leq x \leq 0.5$) perovskite nanostructures. J Magn Magn Mater 465:48–57. https://doi.org/10.1016/j.jmmm.2018.05.094
71. Kotia A, Rajkhowa P, Rao GS, Ghosh SK (2018) Thermophysical and tribological properties of nanolubricants: a review. Heat Mass Transf 54(11):3493–3508. https://doi.org/10.1007/s00231-018-2351-1
72. Sukkar KA, Karamalluh AA, Jaber TN (2019) Rheological and thermal properties of lubricating oil enhanced by the effect of CuO and $TiO_2$ nano-additives. Al-Khwarizmi Eng J 15(2):24–33. https://doi.org/10.22153/kej.2019.12.002
73. Mokarian M, Ameri E (2022) The effect of $Mg(OH)_2$ nanoparticles on the rheological behavior of base engine oil SN500 HVI and providing a predictive new correlation of nanofluid viscosity. Arab J Chem 15(6):103767. https://doi.org/10.1016/j.arabjc.2022.103767
74. Birleanu C, Pustan M, Cioaza M, Molea A, Popa F, Contiu G (2022) Effect of TiO2 nanoparticles on the tribological properties of lubricating oil: an experimental investigation. Sci Rep 12:5201. https://doi.org/10.1038/s41598-022-09245-2
75. Liu X, Xu N, Li W, Zhang M, Lou W, Wang X (2017) Viscosity modification of lubricating oil based on high-concentration silica nanoparticle colloidal system. J Dispersion Sci Technol 38(9):1360–1365. https://doi.org/10.1080/01932691.2016.1220319
76. Kumar Chaurasia S, Kumar Singh N, Kumar Singh L (2020) Friction and wear behavior of chemically modified Sal (Shorea Robusta) oil for bio based lubricant application with effect of CuO nanoparticles. Fuel 282:118762. https://doi.org/10.1016/j.fuel.2020.118762
77. HemmatEsfe M, Saedodin S, Rejvani M, Shahram J (2017) Experimental investigation, model development and sensitivity analysis of rheological behavior of ZnO/10W40 nano-lubricants for automotive applications. Physica E 90:194–203. https://doi.org/10.1016/j.physe.2017.02.015
78. Amjad M, Zehra I, Nadeem S, Abbas N, Saleem A, Issakhov A (2020) Influence of Lorentz force and induced magnetic field effects on Casson micropolar nanofluid flow over a permeable curved stretching/shrinking surface under the stagnation region. Surf Interfaces 21:100766. https://doi.org/10.1016/j.surfin.2020.100766
79. Choudhary R, Khurana D, Kumar A, Subudhi S (2017) Stability analysis of $Al_2O_3$/water nanofluids. J Exp Nanosci 12(1):140–151. https://doi.org/10.1080/17458080.2017.1285445
80. Abdul-Munaim AM, Holland T, Sivakumar P, Watson DG (2019) Absorption wavebands for discriminating oxidation time of engine oil as detected by FT-IR spectroscopy. Lubricants 7(3):24. https://doi.org/10.3390/lubricants7030024
81. Le Dréau Y, Dupuy N, Gaydou V, Joachim J, Kister J (2009) Study of jojoba oil aging by FTIR. Anal Chim Acta 642(1):163–170. https://doi.org/10.1016/j.aca.2008.12.001
82. Saxena A, Kumar D, Tandon N, Kaur T, Singh N (2022) Development of vegetable oil-based greases for extreme pressure applications: an integration of non-toxic, eco-friendly ingredients for enhanced performance. Tribol Lett 70(4):108. https://doi.org/10.1007/s11249-022-01651-x


## Publisher's Note